ingegneria sismica
International Journal of Earthquake Engineering
Anno XLIII - Num. 1 - 2026

Construction of intelligent monitoring and early warning system for plant diseases and pests for small farmers and its economic value evaluation in improving control efficiency

Zhenyan Liu[1,#], *Xiaoqing Yuan*[1,#], *Tao Zhang*[1], *Menghua Luo*[1], *Weiqi Song*[1], *Weijie Song*[1], *Hongxu Chen*[2], *Chunjing Yang*[2], *Wenjuan Chen*[1], *Yuntong Yang*[1], *Pengbo Gong*[1], *Yong Sun*[1,*] *and Can Hu*[1,*]

[1] Deyang Agricultural College, Deyang 618500, Sichuan, China
[2] Sichuan Agricultural University, Chengdu 611130, Sichuan, China
[#] These authors contributed equally to this work

SUMMARY: *For small farmers' plant protection operation scenarios, this paper constructed an intelligent monitoring and warning system that integrated data collection, pest and disease identification, risk warning and instruction push. The system jointly processes multi-source data such as field images, insect trapping, meteorological parameters and crop growth status. The lightweight visual recognition network and time series risk discrimination model are used to complete the disease and insect pest representation learning and early warning level generation, and the end-to-end collaborative mechanism is used to realize end-side collection and cache, edge screening and identification, and cloud strategy update. The experiment is carried out based on 4260 groups of samples. In the recognition tasks of eight types of common pests and diseases, the accuracy of the system reaches 94.6%, the F1 value is 93.8%, the early warning consensus rate is 91.7%, and the response delay is controlled at 1.9 s. The application results show that the system improves the inspection coverage of small farmers by 28.4%, reduces the response time of treatment by 31.6%, and improves the control efficiency per unit area by 24.9%. Further combined with the calculation of pesticide input, labor cost, production loss and average income per mu, the average net income per mu in a single season increased by 186.3 yuan, and the input-output ratio increased by 19.7%, indicating that the system has deployment value and economic benefits under the condition of decentralized operation.*

Povzetek: Ta članek za male kmete vzpostavlja inteligentni sistem za spremljanje in zgodnje opozarjanje na rastlinske bolezni in škodljivce, ki združuje poljske slike, podatke iz vab za insekte in meteorološke podatke za prepoznavanje ter opozarjanje. Poskus je temeljil na 4260 vzorcih. Natančnost prepoznavanja je dosegla 94,6 %, stopnja skladnosti opozoril 91,7 %, odzivni čas pa 1,9 s. Povprečni neto dobiček na mu v eni sezoni se je povečal za 186,3 juana. Rezultati kažejo, da ima sistem praktično uporabno vrednost pri izboljšanju učinkovitosti zatiranja ter povečanju pridelovalnih prihodkov.

KEYWORDS: *Plant diseases and pests; Intelligent monitoring and early warning; Multi-source sensing; Assessment of economic value*

*drhucan@126.com
https://doi.org/10.65102/is2026076
Published: 30 April, 2026

1 Introduction

With the extension of digital agriculture, mobile terminals and edge computing to field operations, plant disease and insect pest monitoring has shifted from manual inspection to a new form supported by data perception, intelligent identification and early warning. The plant protection activities for small farmers have the characteristics of scattered plots, different crops, uneven monitoring frequency and limited application resources. The identification speed, early warning timeliness and decision-making accuracy will directly affect pesticide input, manual scheduling and income. The intelligent monitoring and early warning system based on field images, insect trapping, meteorological parameters and crop growth status can provide a basis for prevention and control efficiency evaluation and economic value measurement.

Related research has been accumulated in the identification and monitoring of plant pests and diseases. Chen et al. proposed MS-DNet model to enhance the adaptation ability of plant disease recognition in terminal scenarios [1]. Li et al. proposed an improved YOLOv5 method for vegetable disease detection, which improved the target detection effect under complex backgrounds [2]. Zhao et al. studied the automatic insect monitoring system based on DPeNet, and realized the automatic identification and counting of insect pests [3]. She et al. proposed a convolutional neural network method with attention mechanism for real-time fruit fly detection in the orchard trap bottle scene [4]. Ye et al. studied the pine forest pest detection method based on remote sensing images and multi-scale attention UNet, which extended the pest perception path [5]. Terentev et al. reviewed the research progress of hyperspectral remote sensing for early detection of plant diseases, which provided reference for perception modeling [6]. However, there are still three aspects to be deepened in the existing research. First, some methods are mainly based on single image recognition, and it is difficult to incorporate insect condition, weather and crop status into the discriminant link. Second, some systems focus on the output of detection results, and have not yet formed a closed loop of early warning generation, prevention and control instruction push and operation feedback linkage. Third, most studies are based on the recognition accuracy as the main evaluation basis, and less involved in the operation efficiency change and economic income increment in the scenario of small farmers.

Based on the above research basis, this paper constructed a monitoring and early warning system for plant pests and diseases for small farmers, and included the economic value assessment in the improvement of control efficiency into the framework. The main work and contributions of this paper are as follows: (1) The overall architecture of the system is constructed to realize the access and collaborative processing of multi-source monitoring data in the field. (2) An early warning link that integrates lightweight identification network and timing risk discrimination is designed to complete pest identification, level generation and control instruction push. (3) The economic value evaluation method is established, and the response time, operation efficiency, input-output ratio and per mu net income are incorporated into the joint calculation.

2 Literature Review

In recent years, the research on intelligent monitoring of plant diseases and pests has gradually expanded from single image classification to multi-source perception, edge-end collaboration and field early warning linkage. Focusing on disease spot recognition, insect detection, environment perception and treatment assistance, related research has formed a technical chain from vision model to system deployment. Shoaib et al. studied the segmentation and

classification method of tomato leaf images, and used deep learning to extract the disease spot area and determine the category, providing an end-to-end path for leaf-level recognition [7]. Dhaka et al. systematically reviewed the application of Internet of Things and deep learning in plant disease detection, and pointed out that sensor collection, cloud-edge collaboration and lightweight model deployment are becoming important directions for disease monitoring [8]. Sowmiya et al. proposed an IOT-supported disease prediction method, which combined sensing input with improved DRDNN to realize agricultural disease state prediction [9]. Huang et al. proposed YOLO-EP algorithm to detect egg mass of pomelo snails in rice fields, which enhanced the recognition ability of small targets in the field [10]. Tang et al. proposed Improved Pest-YOLO to improve the real-time detection accuracy of pests with the support of channel attention and Transformer encoder [11]. Grijalva et al. studied a sorghum aphid detection model based on deep learning, which verified the applicability of computer vision in pest monitoring [12]. These studies show that pest identification has shifted from static sample classification to detection and counting under complex backgrounds, but most of the work is still dominated by single task output, and the coverage of continuous warning links is limited.

With the development of lightweight networks, feature fusion and interpretable modeling, the structural design of plant disease recognition is further refined. Sharma et al. proposed DLMC-Net to improve the recognition effect of leaf diseases through a deeper lightweight multi-classification network [13]. Quan et al. proposed MS-Net to achieve a good balance between lightweight and recognition accuracy, indicating that model compression in mobile deployment scenarios has practical significance [14]. Dai et al. proposed DFN-PSAN multi-layer deep information fusion network to enhance the interpretability and feature expression ability of disease classification [15]. Rezaei et al. studied the plant disease recognition method in small sample scenarios, and introduced few-shot learning into category discrimination under low-data conditions, expanding the adaptation space of the model in the data-scarce environment [16]. This stage of research makes plant disease recognition no longer limited to high-computing power, full-sample and off-line analysis, but advances to the direction of lightweight deployment, low-sample learning and feature interpretability. However, the evaluation of such methods mainly focuses on accuracy, recall rate and F1 value, and it is still less involved in the prevention and control timing, management organization and input-output correlation of farmers.

At the level of system implementation and field application, the research focus is further extended to spatial positioning, edge end operation and task linkage. Zhou et al. proposed a smartphone application for fixed-point pest management, which combined deep learning recognition with spatial interpolation to realize location-related pest management support [17]. Kargar et al. proposed a low-power edge monitoring system for detecting Halyomorpha halys, indicating that low-power devices can undertake continuous monitoring tasks [18]. Grijalva et al. further studied the detection and counting of winged adult sorghum aphids, which strengthened the practicability of intelligent vision model in dynamic insect monitoring [19]. Chakrabarty et al. proposed an insect and damage detection method for cruciferous crops based on YOLOv5, and realized the joint output of insect body recognition and damage judgment [20]. These studies lay a technical foundation for the pest monitoring system from identification module to early warning application, and also show that a clear calculation process has been formed among image acquisition, edge reasoning, spatial mapping and target counting. The technical routes, application objects and applicable boundaries of related research are shown in Table 1.

Table 1: Summary of related studies on intelligent monitoring of plant pests and diseases.

Reference	Method/System	Data or Object	Main Features	Limitations
Shoaib et al. [7]	Deep segmentation and classification	Tomato leaf images	Balances lesion extraction and category identification	Mainly focused on static leaf recognition, with a relatively short warning chain
Dhaka et al. [8]	Review of IoT and deep learning	Multiple disease detection scenarios	Summarizes sensing, transmission, and deployment pathways	Review-oriented, lacking executable system validation
Sowmiya et al. [9]	IoT + improved DRDNN	Sensor-input disease prediction	Supports state prediction and sensor fusion	Insufficient use of visual information
Huang et al. [10]	YOLO-EP	Rice field egg mass targets	Strengthens small-target detection capability	Recognition objects are relatively single
Tang et al. [11]	Improved Pest-YOLO	Pest images	Combines attention mechanism with Transformer	Weak in multi-source collaborative modeling
Grijalva et al. [12]	Deep learning visual model	Sorghum aphids	Supports pest detection	Lacks warning and operation linkage
Sharma et al. [13]	DLMC-Net	Leaf disease images	Lightweight multi-classification modeling	Limited description of system deployment
Quan et al. [14]	MS-Net	Plant disease recognition	Balances accuracy and lightweight design	Limited support for scenario linkage
Dai et al. [15]	DFN-PSAN	Disease classification data	Multi-level feature fusion and interpretability	Economic evaluation was not included
Rezaei et al. [16]	Few-shot learning	Low-sample disease recognition	Adapts to small-sample conditions	Focuses on recognition only, without a warning process
Zhou et al. [17]	Mobile application + spatial interpolation	Fixed-point pest management	Combines location information with recognition results	Edge collaboration remains shallow
Kargar et al. [18]	Low-power edge monitoring system	Halyomorpha halys	Emphasizes continuous monitoring and low-power operation	Limited coverage of recognition categories
Grijalva et al. [19]	Intelligent visual counting model	Winged aphids	Supports joint output of detection and counting	Lacks multimodal inputs
Chakrabarty et al. [20]	YOLOv5 detection	Cruciferous crop insects	Simultaneously outputs pest and	Economic value estimation was not

	framework	and damage	damage information	included

As shown in Table 1, the existing research has covered many directions such as leaf disease classification, insect target detection, mobile terminal recognition, low-power edge monitoring and low-sample learning, indicating that the computational basis of intelligent monitoring of plant diseases and pests is constantly improving. However, from the perspective of system construction, most researches still focus on single-link modeling, lack of unified representation among image, insect condition, weather and crop status, and the continuous mapping from recognition results to warning level, control instruction and operation feedback is not complete. When facing small farmers, the system not only needs to maintain recognition accuracy, but also needs to take into account terminal deployment, edge-end collaboration, early warning timeliness and income calculation. Based on this, this paper builds an intelligent monitoring and early warning system for plant diseases and pests for small farmers on the basis of absorption of existing research results, which integrates multi-source perception, recognition modeling, early warning generation, side-end collaboration and economic value assessment into the same technical framework to enhance the application adaptation ability of the system under decentralized operation conditions.

3 Research Methods

3.1 Overall architecture of intelligent monitoring and early warning system for plant diseases and pests

In terms of system structure design, the overall framework uses end-side acquisition, edge screening, cloud fusion and feedback closed-loop collaborative operation. The terminal side is responsible for continuously collecting field visual information and environmental parameters, and completing compression coding and local caching. A lightweight recognition network was deployed on the edge side to quickly screen disease spots, insects and abnormal growth features, and output candidate categories and confidence scores. The cloud side receives the key frames and intermediate features uploaded by the edge, and combines the historical insect situation, meteorological changes and crop stage information to generate the risk score, which is then mapped by the early warning service module to the control level, application period and operation object. For multiple observations of the same plot in different time Windows, the system uses sliding time Windows to organize monitoring events, so that the recognition results are transformed from single-frame judgment to continuous risk trajectories, so as to reduce the fluctuation caused by accidental noise. As shown in Figure 1, the overall architecture of the system is composed of data acquisition layer, edge identification layer, cloud fusion analysis layer and push feedback layer. All layers operate collaboratively through feature flow and decision flow, forming a complete closed loop of monitoring, identification, early warning and execution.

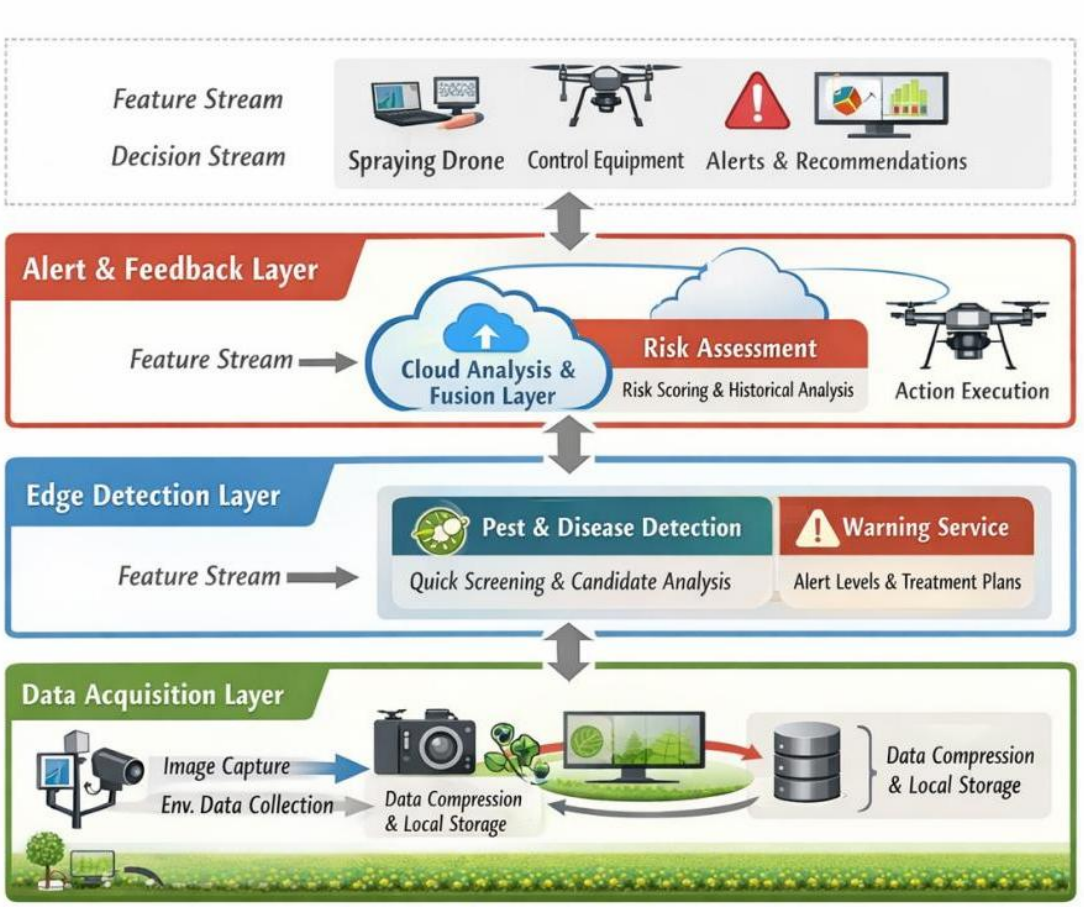

Figure 1: General architecture of intelligent monitoring and early warning system for plant pests and diseases.

Multi-source observations need to complete the unified feature expression before entering the risk discrimination module. To this end, this paper sets independent coding functions for different modal inputs and forms time features through weighted fusion, which is calculated as shown in Equation (1).

$$z_t = \sum_{k=1}^{K} \alpha_k \, \phi_k(x_{k,t}) \tag{1}$$

Here, $x_{k,t}$ represents the input data of the k type of monitoring source at time t; Let ϕ_k denote the feature encoding function of the corresponding modality. α_k represents the weight of the modality in the fusion process. K represents the total number of input modes; Let z_t denote the fused feature vector at time t. The function of equation (1) is to map the image, insect situation, meteorological and crop status uniformly into the same feature space, which provides a consistent data representation for subsequent risk calculation.

After obtaining the fusion features, the system further combines the current observation and historical state to calculate the pest risk score, so that the warning results can reflect the continuous evolution characteristics instead of relying only on the single identification results. The risk scoring process is shown in Equation (2).

$$r_t = \sum_{h=0}^{H-1} \beta_h \ f(z_{t-h}, m_{t-h}) \tag{2}$$

Here, r_t represents the pest risk score at time t. H is the length of the sliding time window; Let β_h denote the weight coefficient corresponding to the h historical moment. $f(\cdot)$ represents the joint mapping function between the observed feature and the historical state; Let z_{t-h} denote the fused feature at time $t-h$. m_{t-h} represents the cumulative monitoring state at time $t-h$ The function of formula (2) is to perform weighted aggregation of multiple observations in the sliding time window, and combine the current observation results with the historical monitoring memory to form a continuous risk estimation, so that the system can identify two types of risk changes: short-term mutation and continuous accumulation.

In order to facilitate the terminal implementation and mobile terminal push, the system also needs to convert the continuous risk value into discrete warning levels, and generate the prevention and treatment suggestions corresponding to the levels synchronously. The mapping mode of early warning output is shown in Formula (3).

$$y_t = \mathcal{G}(u_t, d_t) \tag{3}$$

where y_t represents the output of the warning level at time t; $\mathcal{G}(\cdot)$ represents the warning mapping function; u_t represents the continuous risk score at the current time. d_t represents the auxiliary decision information related to the plot, including crop category, pest type and plot threshold template. The function of equation (3) is to convert the continuous risk score into executable level information and generate a uniform output interface for application period, operation object and control priority.

The overall architecture of the system thus formed has clear computing boundaries and deployment levels. The edge side undertakes fast screening and low-latency reasoning, the cloud side completes multi-source fusion, risk assessment and strategy update, and the feedback layer transmits the early warning results back to the farmer terminal and records the execution results. The design not only retains the sensitivity of the visual recognition model to the representation of pests and diseases, but also enhances the response ability of the system to environmental changes, historical trends and plot differences. It provides a unified data structure and operation basis for subsequent identification accuracy analysis, early warning effectiveness comparison and economic value assessment.

3.2 Multi-source monitoring data collection and pest identification modeling

Before the multi-source monitoring data enters the identification model, the system organizes the original observations by plot unit and time window. Each monitoring sample includes leaf images, insect trapping images, temperature and humidity, rainfall, wind speed, soil moisture content and crop growth status. The image data is collected by the field camera and mobile phone terminal, and the environmental data is periodically reported by the edge sensor node. In order to ensure the consistency of data from different sources at the same calculation time, the system uses 6 hours as the basic window to complete time alignment, performs neighborhood imputation on missing values, and truncates and marks abnormal values. After preprocessing, the multi-source observations of the i plot at time$t$ are represented as a collection of samples, as shown in Equation (4).

$$X_i^t = \{I_t, P_t, E_t, G_t\} \tag{4}$$

Here, I_t represents the leaf image, P_t represents the insect trapping image, E_t represents the environment sequence, and G_t represents the crop state vector. The function of Equation (4) is to unify the observations from different acquisition ports in the same time window into the land-level sample structure and provide consistent input for subsequent multi-source collaborative identification.

In the smallholder scenario, pest and disease representations are not determined by a single image. The color, texture and boundary of leaf disease spots reflect the current state of damage, the number of insects in the trapping device corresponds to the intensity of insect infestation, the change of temperature, humidity and rainfall reflect the expansion condition, and the crop growth period affects the sensitive zone of different diseases and pests. To this end, the system uses dual vision branch and temporal environment branch to complete heterogeneous data expression. Leaf images and insect images are firstly entered into the lightweight convolutional encoder to extract local texture, shape boundary and small target features respectively, and then form a unified visual representation through visual splicing mapping. The process is shown in Equation (5).

$$v_t = W_v[\mathrm{GAP}(F_I(I_t)) \,\|\, \mathrm{GAP}(F_P(P_t))] + b_v \tag{5}$$

Here, $F_I(\cdot)$ and $F_P(\cdot)$ represent convolutional encoders for leaf images and insect infestation images, $\mathrm{GAP}(\cdot)$ represents global average pooling, $\|$ represents vector splicing, W_v and b_v represent visual mapping parameters, and vt represents joint visual features. The function of Equation (5) is to compress leaf disease spot information and insect target information into the same visual expression space, so as to avoid the separation of the two types of images before subsequent fusion. The environment sequence enters the gated recurrent unit to extract the features of short-term fluctuation and continuous change, and the crop type, growth period and plot number enter the embedding layer to generate the state representation. The two are combined to form the non-visual features, which are calculated as shown in Equation (6).

$$n_t = \mathrm{GRU}(E_t, n_{t-1}) + W_g\,\mathrm{Emb}(G_t) + b_g \tag{6}$$

Here, n_t represents the non-visual features at time t, $\mathrm{GRU}(\cdot)$ represents the environment temporal coding unit, n_{t-1} represents the hidden state at the previous time, $\mathrm{Emb}(\cdot)$ represents the state embedding function, and W_g and b_g represent the mapping parameters. The function of Equation (6) is to incorporate environmental fluctuations and crop status into the same state link, so that the model can distinguish the performance differences of the same kind of disease spots under different meteorological conditions and different growth periods in the recognition stage.

There are obvious differences in dimensions and statistical distribution between different modalities, and direct splicing will weaken the role of environmental factors and state factors in the recognition process. In order to reduce the inter-modal shift, the visual features and non-visual features are linearly projected and normalized, and then the attention weight is used to dynamically fuse them to obtain a unified recognition vector. The projection process is written as Equation (7).

$$q_t^m = \mathrm{LN}(W_m h_t^m + b_m), \quad h_t^m \in \{v_t, n_t\} \tag{7}$$

Here, h_t^m represents the original feature of the m modality, W_m and b_m represent the linear mapping parameters of the corresponding modality, $LN(\cdot)$ represents the layer normalization, and q_t^m represents the modal representation after unified scaling. The function of Equation (7) is to make the visual branch and the non-visual branch comparable in the same fusion layer. After scale unification, the system no longer directly calculates the fusion weight based on a single modal feature, but takes the interaction term between the modal feature and the global context into the calculation of the attention score. Let qt be the global reference vector at time t, which consists of the mean of the projected features of each modality, and the attention score of the MTH modality at the current time is written as Equation (8).

$$a_t^m = u^\top \tanh\left(V_q q_t^m + U_q q_t + H_q(q_t^m \odot \bar{q}_t) + c_q\right) \tag{8}$$

Here, a_t^m represents the attention score of the m modality at time t, u is the attention parameter vector, V_q, U_q and H_q are trainable mapping matrices, c_q is the bias term, $\odot$ represents element-wise multiplication, and $\bar{q}_t$ represents the global reference feature before fusion. Equation (8) measures the modal information, the global context information and the coupling relationship between the two at the same time, so that the attention scoring no longer stays at the single path mapping level, but can more fully reflect the actual contribution of different monitoring sources in the current plot and the current time window.

After the attention score is obtained, the system further introduces a gating factor to suppress the interference of noise modes on the fusion result. The weighted fusion features after gated normalization are written as Equation (9).

$$z_t = \sum_m \frac{\gamma_t^m \exp(a_t^m/\tau)}{\sum_j \gamma_t^j \exp(a_t^j/\tau)} q_t^m + \sigma\left(W_r q_t + b_r\right) \odot \bar{q}_t \tag{9}$$

Here, z_t represents the final fusion feature at time t, τ represents the temperature coefficient, γ_t^m represents the gating coefficient of the m mode, $\sigma(\cdot)$ represents the Sigmoid activation function, and W_r and b_r represent the residual gating parameters. The gating coefficient is obtained by linear mapping after concatenating the modal features and the global reference features, which is used to control the openness of different modalities in the fusion process. The function of Equation (9) is to make the fusion feature retain not only the dynamic expression after attention weighting, but also the stable information of the global reference vector, so as to reduce the impact of local abnormal observation on the overall recognition result.

As shown in Figure 2, the whole recognition link is sequentially unfolded by data acquisition, preprocessing, branch encoding, feature fusion, and dual-task output. The edge end first performs candidate region screening and low-resolution identification, and the cloud performs fine discrimination and model update on high-risk samples, so as to reduce the transmission burden while ensuring the quality of recognition.

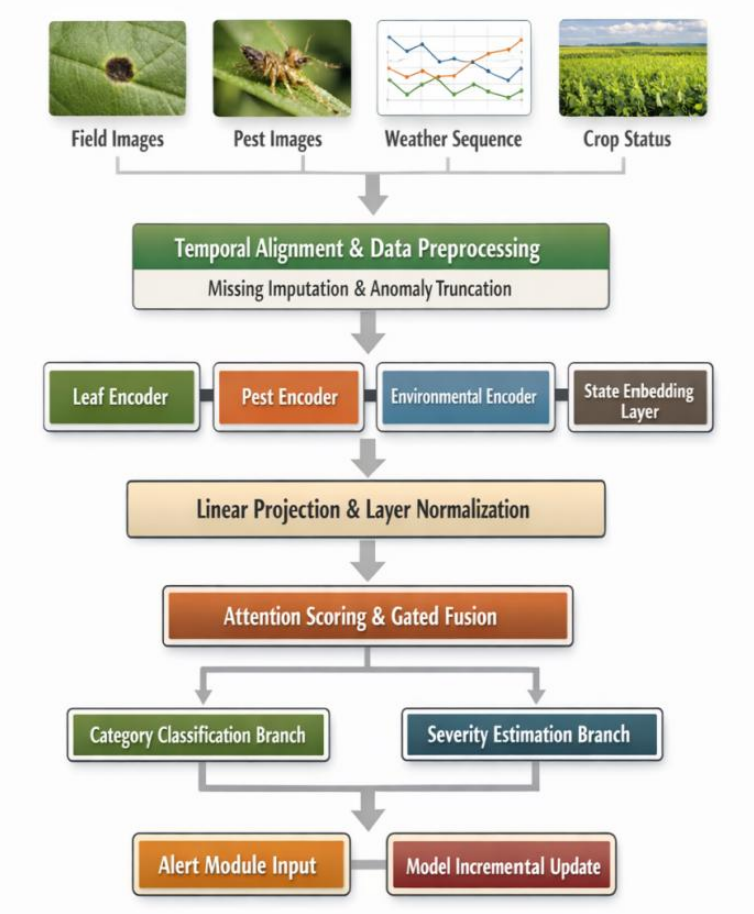

Figure 2: Modeling process of multi-source monitoring data collection and pest identification.

In the identification output stage, the system uses the joint objective to complete the classification of pests and diseases and the occurrence intensity estimation at the same time, and the parameter constraints are incorporated into the same optimization process. The training objective is written as Equation (10).

$$L = \lambda_1 L_{cls} + \lambda_2 \|\hat{s}_t - s_t\|_1 + \lambda_3 \|\Theta\|_2^2 \tag{10}$$

Here, L represents the total model loss, L_{cls} represents the weighted classification loss, $\hat{s}_t$ represents the predicted strength, s_t represents the true strength label, Θ represents all trainable parameters, and λ_1, λ_2, and λ_3 represent the loss weights. The function of Equation (10) is to unify category recognition, intensity estimation and parameter regularization constraints into the same training framework, so that the model can maintain a relatively stable response to the insect grade, disease spot coverage and slight abnormal changes while maintaining the clarity of classification boundaries. The multi-source identification results thus formed can not only be used as the direct input for the generation of warning levels in the next subsection, but also provide a traceable structured data basis for subsequent prevention and control efficiency assessment and economic value measurement. This closed-loop modeling method consisting of acquisition, labeling, training and writeback enables the recognition module to have continuous learning ability, and also provides basic support for the stable deployment of the system in decentralized business scenarios.

3.3 Intelligent early warning generation and control instruction push mechanism for pests and diseases

In order to complete the early warning generation, the system constructed a computing link composed of risk update, level judgment and instruction matching. The module takes the fusion feature $z_t$and intensity estimate $\hat{s}_t$ output in the previous section as the basic input. At the same time, it introduces the risk stater_{t-1} at the previous time and the current job state vector o_t to generate the risk score at time t in a continuous update manner, and its expression is:

$$r_t = \lambda r_{t-1} + (1-\lambda)\,\sigma(W_z z_t + W_s \hat{s}_t + W_o o_t + b_r) \tag{11}$$

Here, r_t represents the current risk score, r_{t-1} represents the risk state at the last time, λ represents the historical attenuation coefficient, W_z, W_s and W_o are trainable mapping matrices, b_r is the bias term, and $\sigma(\cdot)$ is the activation function. Equation (11) maps the current identification results, occurrence intensity and operating conditions into a unified risk space, and then performs attenuation fusion with the historical risk state, so that the early warning results can not only reflect the actual intensity of current pests and diseases, but also retain the evolution trend in continuous monitoring, thus enhancing the characterization ability of extended risks.

After obtaining the continuous risk value, the system completes the level mapping according to the crop type, pest type and plot threshold template, and the set of warning levels is set to four categories: low, medium, high and emergency, whose expression is:

$$y_t = \arg\max_c \; 1(T_c^- \le r_t < T_c^+) \tag{12}$$

where y_t represents the output of the warning level at time t, T_c^- and T_c^+ represent the lower and upper bounds of the risk interval at level c, respectively, and $1(\cdot)$ is the indicator function. The function of Equation (12) is to transform the continuous risk value into a discrete level that can be recognized by the terminal, so as to provide a clear input for subsequent disposal action matching.

Subsequently, the push module scores the candidate actions by combining agent inventory, weather window, and human reachability, and outputs the prevention proposal with the highest priority. If the KTH candidate action is denoted as Ak, its matching score is written as:

$$p_k = \eta_1 C_k + \eta_2 D_k + \eta_3 R_k, \quad A^* = \arg\max_k p_k \tag{13}$$

where p_k represents the action priority, C_k represents the resource matching degree, D_k represents the timeliness adaptation degree, R_k represents the risk responsiveness degree, η_1, η_2, and η_3 are the weight coefficients, and A^* represents the final push action. The function of Equation (13) is to unify resource conditions, time constraints and risk level into the same ranking rule, so that different parcels can get differentiated implementation suggestions.

As shown in Figure 3, the whole module is composed of four parts: risk calculation, level generation, action matching and terminal feedback. After receiving the results, the mobile terminal can synchronously display the plot number, pest category, suggested time period and disposal method, and return the execution status after the job is completed for updating the risk memory of the next time period. In this way, the system established a continuous closed loop between the identification results and the actual control, and also provided a traceable data basis for the subsequent control efficiency evaluation and economic value measurement.

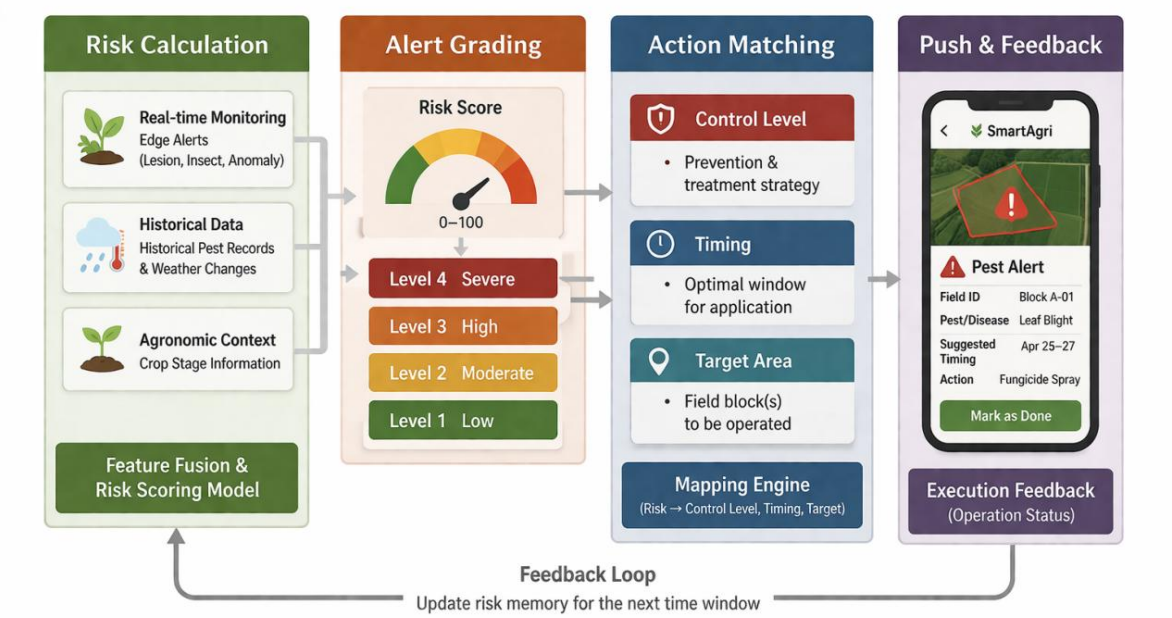

Figure 3: Process of intelligent warning generation and control instruction push for pests and diseases.

The mechanism further transforms the identification results into orderable and executable prevention and control instructions, so that the warning output does not stay at the result prompt level, but can directly correspond to the plot, time period and disposal action. The execution record returned by the terminal can reverse update the risk status, so as to provide continuous data support for subsequent early warning correction, operation efficiency analysis and economic value measurement.

3.4 Module integration and side-end collaboration of intelligent monitoring and early warning system for plant diseases and pests

After pest identification, risk discrimination and control action generation, the system also needs to organize the acquisition terminal, edge node, cloud service and mobile terminal execution entry into a unified operation link, so as to adapt to the actual scene of scattered small farmers' plots, limited terminal performance and obvious fluctuations in communication conditions. Based on this deployment requirement, this paper constructs a module integration and edge-end coordination mechanism, which integrates the monitoring data flow, early warning and discrimination flow, instruction distribution flow and feedback writeback flow into the same scheduling framework, so that the recognition results can be stably transmitted from the plot end to the decision end, and continue to flow back to the model update link after execution.

The system first encapsulates the states that need to be processed on the edge side into a unified task unit, whose expression is:

$$u_t = [z_t, r_t, y_t, o_t, l_t] \tag{14}$$

Here, u_t represents the task unit at time t, z_t represents the recognition fusion feature, r_t represents the risk score, y_t represents the warning level, o_t represents the current job status, and l_t represents the equipment and network load. The function of Equation (14) is to compress the identification results, early warning results and operation status into a unified object, which

is convenient for edge nodes to complete caching, scheduling and uploading according to the same interface.

On this basis, the edge node does not directly send all samples to the cloud, but calculates the upload priority by combining risk level, occurrence intensity, identification confidence and load status. The calculation method is as follows.

$$\xi_t = \rho_1 r_t + \rho_2 s_t + \rho_3 (1 - q_t) + \rho_4 l_t \tag{15}$$

Here, ξ_t represents the upload priority, s_t represents the occurrence intensity estimate, q_t represents the edge identification confidence, and ρ_1 toρ_4 represent the weight parameters. Equation (15) is used to screen samples with high risk, strong occurrence, low confidence and high disturbance, so that the edge side retains the fast response ability, and the cloud side focuses on processing more valuable complex samples.

After the upload priority is obtained, the system completes edge-cloud diversion control according to the threshold, and its routing label is written as follows.

$$a_t = \begin{cases} 1, & \xi_t \geq \tau_e \\ 0, & \xi_t < \tau_e \end{cases} \tag{16}$$

Here, a_t represents the task routing tag,τ_e represents the upload threshold, $a_t = 1$ means that the task enters the cloud precision judgment queue, and a_t means that the task remains at the edge side for local processing. Equation (16) ensures that the system can still maintain low delay operation under the condition of limited bandwidth, while avoiding resource consumption caused by repeated transmission.

After receiving key samples, the cloud further generates executable instructions by combining historical monitoring records, crop stages, weather Windows and inventory constraints. To ensure that the terminal can directly call the result, the system encodes the risk level, action type and time period information into a unified push vector, which is expressed as:

$$c_t = W_c[r_t, y_t, A_k, w_t] + b_c \tag{17}$$

where c_t represents terminal instruction encoding vector, A_k represents candidate prevention action, w_t represents weather window constraint, W_c and b_c represent mapping matrix and bias term, respectively. Equation (17) converts the risk judgment results into message content that can be pushed and executed, so that the mobile terminal can synchronously display the plot number, pest and disease category, suggested time period and disposal method.

In the execution phase, the mobile terminal will send back the completion time, medication information, labor input and review results to the feedback library, and the system will use the feedback results to update the memory state of the plot. The update method is as follows:

$$m_t = \gamma m_{t-1} + (1 - \gamma) F_t \tag{18}$$

Here, m_t represents the updated plot memory state, m_{t-1} represents the risk memory of the last round, F_t represents the terminal feedback vector, and γ represents the memory decay coefficient. The function of Equation (18) is to bring the execution result back into the monitoring link, so that the system can use the historical disposal effect to revise the risk judgment in the next round of warning generation.

The resulting module integration process consists of three consecutive links. In the terminal access stage, the plot number binding, time alignment and field standardization were completed to ensure that the image, insect situation and meteorological data were entered into the same

event table. The edge coordination phase is responsible for cache maintenance, anomaly screening, lightweight inference and routing control, so as to ensure that local results can still be output in weak network environment. The cloud synchronization stage is responsible for complex sample re-judgment, rule update and parameter return, so that the new strategy can be synchronized to the subsequent land parcel tasks. The unified key-value index and asynchronous message mechanism are adopted among each module, and the state table, feature table and feedback table maintain a consistent mapping relationship, so as to reduce the cross-device call overhead and provide a stable data operation basis for subsequent performance analysis, early warning effectiveness comparison and economic value evaluation.

4 Results and discussion

4.1 Comparison of pest identification accuracy and early warning effectiveness

The experiment was carried out based on 4260 groups of field samples, covering common planting scenes of small farmers such as rice, citrus and vegetables, including multi-source information such as disease spot images, insect trapping images, temperature and humidity, rainfall, wind speed, soil moisture content, and crop growth status, involving eight types of common diseases and pests. The data was divided into training set, validation set and test set according to 7:2:1, and the comparative test was completed in the same side-end collaborative environment. In the evaluation stage, the recognition accuracy, F1 value, early warning consensus rate and response time delay are unified to measure the comprehensive performance of the system in recognition accuracy, alarm stability and real-time processing ability, and the data aperture is unified and reliable.

In order to evaluate the recognition Accuracy and early Warning effectiveness of the system in the scenario of small farmers, this paper selects Accuracy, F1, Warning Consistency and Response Delay as the core indicators. The unified test between the proposed method and three types of baselines, MobileNetV3, YOLOv5n and CNN-GRU, is shown in Figure 4.

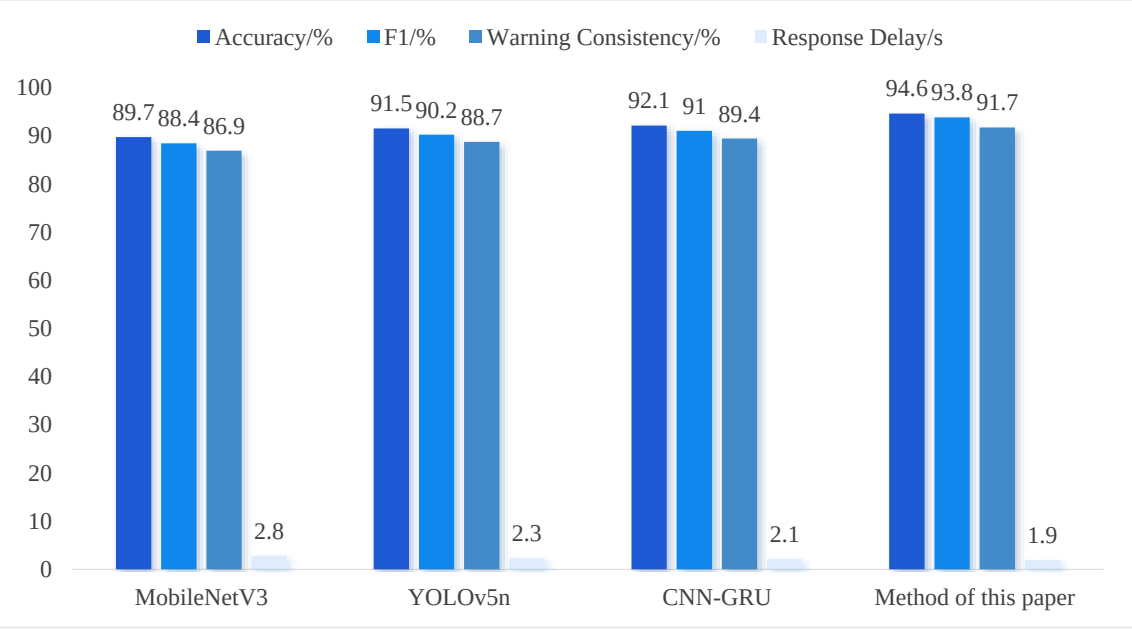

Figure 4: Overall comparison of pest identification accuracy and early warning effectiveness.

The comparison results show that the proposed method achieves the best performance in four indicators, with the recognition accuracy of 94.6%, the F1 value of 93.8%, the early warning consensus rate of 91.7%, and the response delay controlled at 1.9 s. Compared with MobileNetV3, the accuracy, F1 value and early warning consensus rate are increased by 4.9, 5.4 and 4.8 percentage points, respectively, and the response delay is shortened by 0.9 s. Compared with YOLOv5n, the three accuracy indicators are increased by 3.1, 3.6 and 3.0 percentage points respectively, and the response delay is shortened by 0.4 s. Compared with CNN-GRU, the accuracy, F1 value and early warning consensus rate are still increased by 2.5, 2.8 and 2.3 percentage points, respectively, and the response delay is shortened by 0.2 s. It shows that multi-source input, temporal risk discrimination, and edge-end collaborative links can simultaneously enhance the consistency of category recognition, intensity representation, and alarm output in complex field backgrounds.

4.2 Monitoring stability analysis under different crops and types of pests and diseases

In order to evaluate the monitoring stability of the system under different crops and pest types, this paper took 8 types of objects with high frequency in 4260 groups of samples as the analysis unit, covering rice planthopper, rice blight, citrus canker, citrus leaf leaf-creeping moth, vegetable downy mildew, vegetable aphid, rice blast disease and citrus starspider. Moreover, the F1 value and the warning agreement rate of each model on the test set are uniformly counted, and the results are shown in Figure 5.

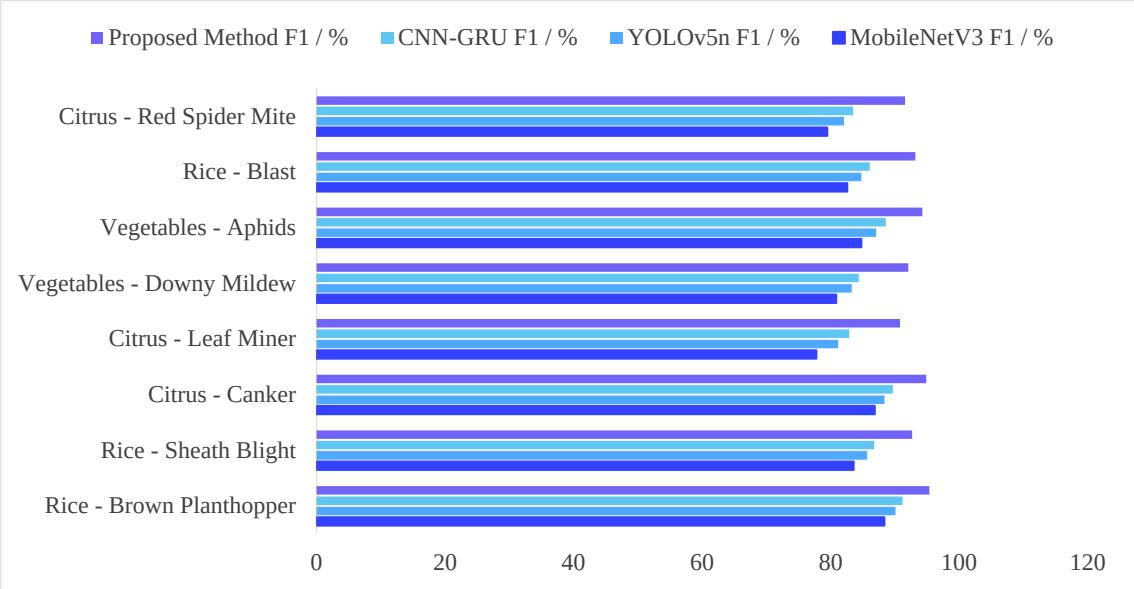

Figure 5: Monitoring stability analysis under different crops and pest and disease types.

The F1 value of the proposed method on eight types of objects is distributed between 90.8%-95.4%, with a fluctuation interval of 4.6 percentage points, while the fluctuation interval of MobileNetV3 is 10.6 percentage points, YOLOv5n and CNN-GRU are 8.9 and 8.3 percentage points, respectively. This indicates that the proposed method maintains a high degree of stability in cross-crop and cross-pest and disease scenarios. Taking the citrus leaf leaf leaf moth as an example, the F1 value of the proposed method is 90.8%, which is 13.0, 9.6 and 7.9 percentage points higher than that of MobileNetV3, YOLOv5n and CNN-GRU, respectively. In the vegetable downy mildew scenario, the proposed method reaches 92.1%, which is 11.2, 8.8 and 7.7 percentage points higher than the three baselines, respectively. The results show that the

multi-source fusion coding can weaken the disturbance caused by leaf reflection, blurred boundary of disease spots and insect occlusion, and the temporal environment branch and risk memory compensate for the category shift caused by single frame texture loss. After repeating the experiment five times and performing paired t-test, the differences of each category reached a significant level, indicating that the system has a stable cross-category monitoring ability.

4.3 Influence analysis of multi-source input and early warning link on system performance

In order to analyze the influence of multi-source input and early warning link on system performance, this paper sets five configurations: image only, image plus insect condition, image plus weather, image plus insect condition and weather, and complete early warning link. Accuracy, F1, Warning Consistency and Response Delay are compared under the same training rounds, the same test set and the same edge hardware conditions, and the results are shown in Figure 6.

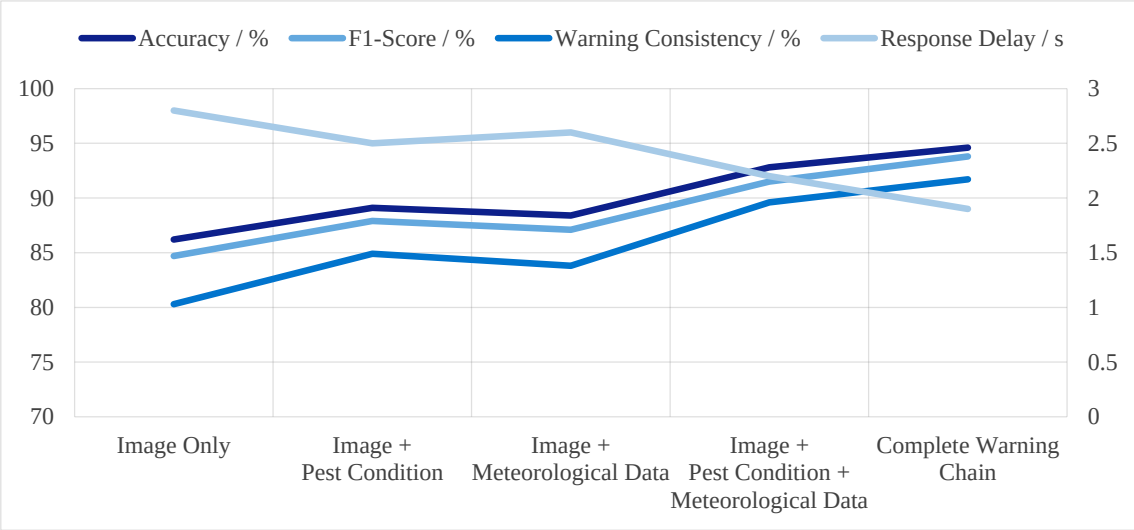

Figure 6: Analysis of the impact of multi-source inputs and warning links on system performance.

When only images are input, the accuracy, F1 and early warning consensus rate are 86.2%, 84.7% and 80.3%, respectively. After adding insect trapping, it increased to 89.1%, 87.9% and 84.9%; When meteorological parameters were added alone, the results were 88.4%, 87.1% and 83.8%, respectively, indicating that the contribution of insect situation information to short-term alarm discrimination was more direct. When images, insect conditions and meteorology enter the fusion layer at the same time, the three indicators further rise to 92.8%, 91.5% and 89.6%, and the complete warning link reaches 94.6%, 93.8% and 91.7%, which is 8.4, 9.1 and 11.4 percentage points higher than that of image-only configuration, respectively. The response time is reduced from 2.8 seconds to 1.9 seconds. The improvement of task scheduling efficiency on the edge side is more obvious. The results show that early warning feedback, risk memory and edge-cloud diversion are not additional processes, but directly participate in risk update and action generation. After repeating the experiment five times and performing paired t-test, the main differences among different configurations reach significant levels, indicating that multi-source inputs and closed-loop links have a stable support effect on system performance.

4.4 Improvement of control timeliness and evaluation of operation efficiency for small farmers

In order to evaluate the improvement of prevention and control timeliness and the change of operation efficiency of the system in the scenario of small farmers, the test plots were consecutively counted according to five observation stages before deployment, 2 weeks, 4 weeks, 6 weeks and 8 weeks, and the increase of inspection coverage rate, the decrease of treatment response time and the increase of operation efficiency per unit area were uniformly recorded. And the comparative analysis is completed under the same terminal configuration, the same network conditions and the same operation rules, and the results are shown in Figure 7.

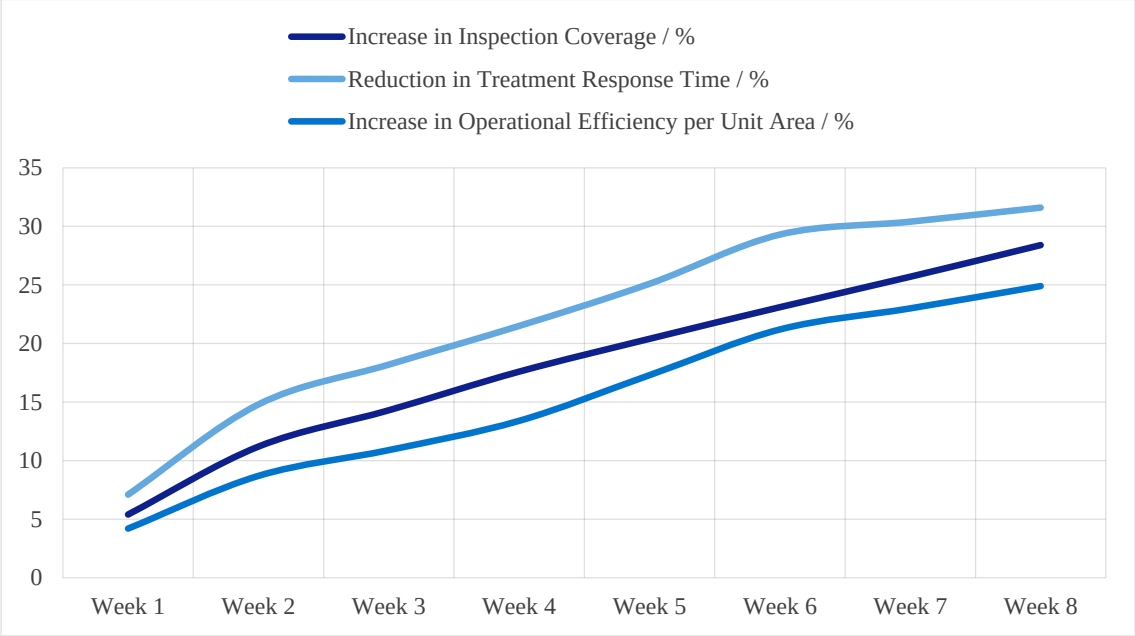

Figure 7: timeliness improvement and operational efficiency evaluation of smallholder farmers.

After the deployment of the system, all indicators were significantly improved, and the inspection coverage rate was gradually improved from the baseline state, reaching 28.4% in the 8th week. The reduction of response time was 14.8% in the second week, 29.3% in the sixth week, and 31.6% in the eighth week. The control efficiency per unit area increased from 8.7% to 24.9%. This change shows that the closed-loop link composed of mobile terminal task push, edge screening and cloud re-judgment reduces the waiting time between the detection of anomalies and the execution of disposal, and reduces the labor consumption caused by repeated field inspection and ineffective application. Compared with the traditional manual inspection method, the system formed a higher task arrival rate and a more stable operation rhythm in the eighth week, which made the high-risk parcels enter the disposal queue first, and the resource scheduling was more concentrated. Five repeated experiments were further carried out, and paired t-test was used to verify the differences in each stage. The results reached a significant level in the main indicators, indicating that the system has stable improvement ability of timeliness and operation efficiency gain under the condition of small farmers' decentralized operation. From the perspective of calculation implementation, the terminal side first packaged the image, insect situation and meteorological events into a plot level task package, the edge node completed the rapid diversion according to the risk threshold, and the cloud revised the action priority according to historical feedback. Therefore, the alarm results could be directly converted into the application time, review sequence and manual arrival arrangement, and the

high-risk samples were captured earlier in the subsequent rounds. The overall operation is more stable, more accurate scheduling.

4.5 Analysis of ablation experiments

In order to verify the actual contribution of the modules in the intelligent monitoring and early warning system of plant diseases and pests, this section carries out ablation experiments around three parts: multi-source fusion coding, time series risk update, and edge-cloud co-scheduling. By comparing the performance of the complete model with the variant with different modules removed on the test set, the influence of each component unit on the recognition accuracy, early warning agreement rate and response delay can be quantified, and the effectiveness of the system structure design can be illustrated. Different model variants are defined as follows: the complete model includes a multi-source fusion coding module, a timing risk update module and an edge-cloud collaborative scheduling module. After removing the multi-source fusion coding, only the main branch of the image and the basic environment input were retained. After removing the temporal risk update, the early warning results were directly generated from the current identification output. After removing edge-cloud co-scheduling, all tasks are processed in a single path, and risk triage and feedback writeback are no longer performed. The comparison results of each model are shown in Table 2.

Table 2: Results of ablation experiments.

Model Version	Accuracy / %	F1-Score / %	Warning Consistency / %	Response Delay / s
Full Model	94.6	93.8	91.7	1.9
Without Multi-source Fusion Encoding	91.8	90.9	88.9	2.2
Without Temporal Risk Updating	92.4	91.6	88.6	2.1
Without Edge-Cloud Collaborative Scheduling	93.1	92.0	89.4	2.6
Without the Above Three Modules	89.7	87.8	84.5	3.0

The complete model achieves the best performance in Accuracy, F1 and Warning Consistency, while maintaining the lowest response delay. After removing the multi-source fusion coding, the accuracy decreased from 94.6% to 91.8%, and the F1 value decreased from 93.8% to 90.9%, indicating that the category boundary and intensity characteristics were clearer after the insect condition, weather and crop status were involved in the representation. After removing the temporal risk update module, the warning consensus rate decreases from 91.7% to 88.6%, indicating that the continuous risk memory can weaken the amplification effect of single frame misjudgment on the alarm results. After removing edge-cloud co-scheduling, the response delay increases from 1.9 s to 2.6 s, and the warning consensus rate also decreases, which indicates that task offloading, edge screening and cloud re-judgment support the output ability. If the three types of mechanisms are weakened at the same time, the system performance decreases most obviously, which indicates that the modules are not simply superimposed, but form a mutually supporting computing relationship in the identification, early warning and execution links. Ablation results show that the multi-source fusion coding enhances the discrimination of pest representation, the temporal risk update improves the stability of early warning output, and the edge-cloud co-scheduling improves the task processing efficiency and

on-site adaptation ability. It also verifies the technical effectiveness and structural rationality of the proposed method in the scenario of small farmers.

4.6 Economic value evaluation in improving control efficiency

In order to evaluate the economic value of the system in improving the efficiency of prevention and control, this paper quantified the inspection records, application accounts, labor input, production reduction estimation and average income per mu before and after deployment, and carried out comparative calculation under the same crop structure, similar meteorological conditions and consistent management caliber. The measured indicators include pesticide input, labor cost, loss of production reduction, net income per mu and input-output ratio, and the results are shown in Table 3.

Table 3: Measurement results of economic value in improving prevention and control efficiency.

Indicator	Before Deployment	After Deployment	Change
Pesticide Input / (CNY·mu^{-1})	186.7	171.4	-15.3
Labor Cost / (CNY·mu^{-1})	243.5	212.6	-30.9
Yield Loss / (CNY·mu^{-1})	318.2	191.1	-127.1
Net Income per mu / (CNY·mu^{-1})	946.8	1133.1	+186.3
Input-Output Ratio	2.74	3.28	+19.7%

After the deployment of the system, the pesticide input per unit area of small farmers was reduced from 186.7 yuan to 171.4 yuan, the labor cost was reduced from 243.5 yuan to 212.6 yuan, and the loss of production reduction was reduced from 318.2 yuan to 191.1 yuan, indicating that the identification results, early warning levels and disposal instructions had been transformed into economic benefits that could be measured. Compared with the traditional inspection method, the average net income per mu under the assistance of the system increased from 946.8 yuan to 1133.1 yuan, an increase of 186.3 yuan per season, and the input-output ratio increased from 2.74 to 3.28, an increase of 19.7%. This result is consistent with the above timeliness analysis, indicating that the improvement of inspection coverage and the reduction of treatment response time directly change the rhythm of resource allocation, make high-risk plots enter the treatment queue earlier, and reduce the drug accumulation and yield loss caused by delayed disposal. From the perspective of calculation implementation, the job records reported by the mobile terminal, the risk log generated by the edge node and the action template output by the cloud are uniformly written into the benefit assessment module, and then the cost collection and benefit calculation are carried out according to the plot number. Therefore, the economic indicators are not independent estimation results, but are jointly driven by the identification, early warning, execution and feedback links. After five times of repeated measurement and paired t-test, the differences of various economic indicators reached a significant level, indicating that the system not only improved the efficiency of monitoring and disposal of pests and diseases, but also formed a stable income increment under the condition of decentralized management. From the perspective of indicator linkage relationship, after the increase of early warning consistency rate, the number of repeated reviews decreased, the edge end screening reduced invalid uploads, and the cloud rejudgment improved the matching degree of drug application period, so that the drug investment, manual organization and production reduction control formed a closer collaborative relationship, and the economic value was expressed as the comprehensive effect of accurate monitoring, timely scheduling and synchronous improvement of revenue recovery.

4.7 Discussion

The above experiments show that the intelligent monitoring and early warning system of plant diseases and pests constructed in this paper has gains in four levels: identification, early warning, timeliness and income. In the overall test, the recognition accuracy of the system reaches 94.6%, the F1 value is 93.8%, the early warning consensus rate is 91.7%, and the response delay is controlled at 1.9 s. In the cross-crop and pest type analysis, the F1 fluctuation interval of the proposed method is only 4.6 percentage points, which is significantly smaller than that of the baseline model. After 8 weeks of deployment, the inspection coverage rate increased by 28.4%, the treatment response time shortened by 31.6%, the operation efficiency per unit area increased by 24.9%, the average net income per mu increased by 186.3 yuan per season, and the input-output ratio increased by 19.7%. These results show that multi-source sensing input, temporal risk update, edge-cloud co-scheduling and feedback write-back are not decentralized modules, but jointly support continuous monitoring, rapid disposal and income recovery in the scenario of small farmers in the unified computing link.

5 Conclusion

5.1 Research Conclusions

In this paper, a monitoring and warning system integrating multi-source perception, identification modeling, risk warning, instruction push and feedback writeback is constructed for the plant protection scenario of small farmers. The system takes field images, insect trapping, meteorological parameters and crop growth status as input, and completes the identification through lightweight visual network, time series risk update and edge-cloud collaborative link. Experiments show that in 4260 groups of samples and 8 kinds of pest and disease tasks, the accuracy of the system reaches 94.6%, the F1 value is 93.8%, the warning consensus rate is 91.7%, and the response delay is controlled at 1.9 seconds. After deployment, the inspection coverage rate is increased by 28.4%, the treatment response time is shortened by 31.6%, the operation efficiency per unit area is increased by 24.9%, and the net income per mu is increased by 186.3 yuan, which reflects the practicability and application value.

5.2 Limitations and Future research Directions

Although the system has achieved stable results in identification, early warning and income calculation, the current training samples are still mainly single-season data and limited plots, and the ability of cross-regional migration and cross-crop reuse still needs to be strengthened. For extreme weather disturbances, weak signal insect conditions and low-frequency disease spots, the model representation still relies on high-quality inputs, and there is also a certain computational pressure at the edge end under the condition of high concurrent uploads. The following research can be carried out in four directions: lightweight network compression, adaptive threshold update, multi-seasonal incremental learning and multi-regional data collaborative modeling. The pharmacy inventory, manual scheduling and revenue prediction can be integrated into the unified decision-making link, so that the identification, early warning, execution and writeback can form a tighter data closed loop. The continuous operation ability, deployment flexibility and result interpretation ability of the system are further enhanced.

References

[1] Chen W, Chen J, Duan R, et al. MS-DNet: A mobile neural network for plant disease identification[J]. Computers and Electronics in Agriculture, 2022, 199: 107175. https://doi.org/10.1016/j.compag.2022.107175

[2] Li J, Qiao Y, Liu S, et al. An improved YOLOv5-based vegetable disease detection method[J]. Computers and Electronics in Agriculture, 2022, 202: 107345. https://doi.org/10.1016/j.compag.2022.107345

[3] Zhao N, Zhou L, Huang T, et al. Development of an automatic pest monitoring system using a deep learning model of DPeNet[J]. Measurement, 2022, 203: 111970. https://doi.org/10.1016/j.measurement.2022.111970

[4] She J, Zhan W, Hong S, et al. A method for automatic real-time detection and counting of fruit fly pests in orchards by trap bottles via convolutional neural network with attention mechanism added[J]. Ecological Informatics, 2022, 70: 101690. https://doi.org/10.1016/ j.ecoinf.2022.101690

[5] Ye W, Lao J, Liu Y, et al. Pine pest detection using remote sensing satellite images combined with a multi-scale attention-UNet model[J]. Ecological Informatics, 2022, 72: 101906. https://doi.org/10.1016/j.ecoinf.2022.101906

[6] Terentev A, Dolzhenko V, Fedotov A, et al. Current state of hyperspectral remote sensing for early plant disease detection: A review[J]. Sensors, 2022, 22(3): 757. https://doi.org/10.3390/s22030757

[7] Shoaib M, Hussain T, Shah B, et al. Deep learning-based segmentation and classification of leaf images for detection of tomato plant disease[J]. Frontiers in plant science, 2022, 13: 1031748.https://doi.org/10.3389/fpls.2022.1031748

[8] Dhaka V S, Kundu N, Rani G, et al. Role of internet of things and deep learning techniques in plant disease detection and classification: A focused review[J]. Sensors, 2023, 23(18): 7877.https://doi.org/10.3390/s23187877

[9] Sowmiya M, Krishnaveni S. IoT enabled prediction of agriculture's plant disease using improvedϖ quantum whale optimization DRDNN approach[J]. Measurement: Sensors, 2023, 27: 100812.https://doi.org/10.1016/j.measen.2023.100812

[10] Huang Y, He J, Liu G, et al. YOLO-EP: A detection algorithm to detect eggs of Pomacea canaliculata in rice fields[J]. Ecological Informatics, 2023, 77: 102211. https://doi.org/10.1016/j.ecoinf.2023.102211

[11] Tang Z, Lu J, Chen Z, et al. Improved Pest-YOLO: Real-time pest detection based on efficient channel attention mechanism and transformer encoder[J]. Ecological Informatics, 2023, 78: 102340.https://doi.org/10.1016/j.ecoinf.2023.102340

[12] Grijalva I, Spiesman B J, McCornack B. Computer vision model for sorghum aphid detection using deep learning[J]. Journal of Agriculture and Food Research, 2023, 13: 100652.https://doi.org/10.1016/j.jafr.2023.100652

[13] Sharma V, Tripathi A K, Mittal H. DLMC-Net: Deeper lightweight multi-class classification model for plant leaf disease detection[J]. Ecological informatics, 2023, 75: 102025.https://doi.org/10.1016/j.ecoinf.2023.102025

[14] Quan S, Wang J, Jia Z, et al. MS-Net: a novel lightweight and precise model for plant disease identification[J]. Frontiers in Plant Science, 2023, 14: 1276728. https://doi.org/10.3389/fpls.2023.1276728

[15] Dai G, Tian Z, Fan J, et al. DFN-PSAN: Multi-level deep information feature fusion extraction network for interpretable plant disease classification[J]. Computers and Electronics in Agriculture, 2024, 216: 108481. https://doi.org/10.1016/j.compag.2023.108481

[16] Rezaei M, Diepeveen D, Laga H, et al. Plant disease recognition in a low data scenario using few-shot learning[J]. Computers and electronics in agriculture, 2024, 219: 108812. https://doi.org/10.1016/j.compag.2024.108812

[17] Zhou C, Lee W S, Zhang S, et al. A smartphone application for site-specific pest management based on deep learning and spatial interpolation[J]. Computers and Electronics in Agriculture, 2024, 218: 108726. https://doi.org/10.1016/j.compag.2024.108726

[18] Kargar A, Zorbas D, Tedesco S, et al. Detecting Halyomorpha halys using a low-power edge-based monitoring system[J]. Computers and Electronics in Agriculture, 2024, 221: 108935.https://doi.org/10.1016/j.compag.2024.108935

[19] Grijalva I, Adams H B, Clark N, et al. Detecting and counting sorghum aphid alates using smart computer vision models[J]. Ecological Informatics, 2024, 80: 102540. https://doi.org/10.1016/j.ecoinf.2024.102540

[20] Chakrabarty S, Shashank P R, Deb C K, et al. Deep learning-based accurate detection of insects and damage in cruciferous crops using YOLOv5[J]. Smart Agricultural Technology, 2024, 9: 100663.https://doi.org/10.1016/j.atech.2024.100663